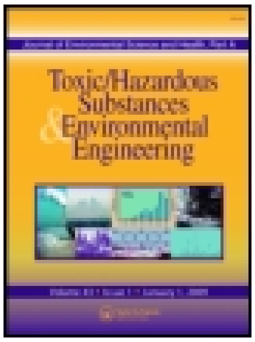

Taylor & Francis
Taylor & Francis Group

Journal of Environmental Science and Health, Part A
Toxic/Hazardous Substances and Environmental Engineering

ISSN: 1093-4529 (Print) 1532-4117 (Online) Journal homepage: https://www.tandfonline.com/loi/lesa20

Thermophilic anaerobic digestion of cattail and hydrothermal carbonization of the digestate for co-production of biomethane and hydrochar

Bo Zhang, Gail Joseph, Lijun Wang, Xin Li & Abolghasem Shahbazi

To cite this article: Bo Zhang, Gail Joseph, Lijun Wang, Xin Li & Abolghasem Shahbazi (2019): Thermophilic anaerobic digestion of cattail and hydrothermal carbonization of the digestate for co-production of biomethane and hydrochar, Journal of Environmental Science and Health, Part A, DOI: 10.1080/10934529.2019.1682367

To link to this article: https://doi.org/10.1080/10934529.2019.1682367

Published online: 25 Oct 2019.

Submit your article to this journal

Article views: 67

View related articles

View Crossmark data

Full Terms & Conditions of access and use can be found at
https://www.tandfonline.com/action/journalInformation?journalCode=lesa20

JOURNAL OF ENVIRONMENTAL SCIENCE AND HEALTH, PART A
https://doi.org/10.1080/10934529.2019.1682367

Thermophilic anaerobic digestion of cattail and hydrothermal carbonization of the digestate for co-production of biomethane and hydrochar

Bo Zhang, Gail Joseph, Lijun Wang, Xin Li, and Abolghasem Shahbazi

Department of Natural Resources and Environmental Design, North Carolina Agricultural and Technical State University, Greensboro, North Carolina, USA

ABSTRACT
Thermophilic anaerobic digestion (AD) of cattail followed by hydrothermal carbonization (HTC) was studied. The intent of the research was to develop agricultural waste-based biorefining technologies for bioenergy production along with value-added products. Cattail was anaerobically digested at 55 °C for 14 days and protein and cellulose components were partially degraded. The average methane yield was 230–280 mL/g volatile solids and the total solids decreased by 33–55%. When the particle size of cattail was reduced from 1 in. to 1 mm, the lag phase was shortened from 1.48 to 0 d. Following the AD process of cattail, the AD digestate was hydrothermally carbonized at 250 °C for 4 h, yielding approximately 6.7–7.5 wt % gaseous products, 64 wt % liquid products and 28 wt % hydrochar. The gaseous products contained >5000 ppm H_2S and liquid products possessed fewer chemicals and higher ratio of phenolic compounds compared to the liquid products from HTC of original cattail. The hydrochar had a higher carbon content (76.8–79.8%) and a higher specific surface area (~10 m^2/g) than those of the feedstock. Hydrochar was further activated by using Na_2CO_3, $NaHCO_3$ and NaCl. The activation process increased the carbon content and specific surface area to 84–93% and 250–630 m^2/g, respectively.

ARTICLE HISTORY
Received 13 August 2019
Accepted 7 October 2019

KEYWORDS
Biogas; methane; particle size; HTC; biochar; micropore; molten salt activation

Introduction

Driven by global population growth, rapid urbanization, changes in diet and economic growth, the human society has shown a rapid increase in demand for food, energy and water (FEW) resources.[1] These three important resources are interlinked in several ways. Agricultural production and food processing are the world's largest consumers of freshwater resources, and more than a quarter of the energy used worldwide is consumed for food production and supply.[2,3] Therefore, an integrated approach to ensure water security, food security and global sustainable agriculture along with energy production is essential. Waste-based integrated biorefinery can be utilized for increasing the resilience of FEW systems. The agricultural industry generates large amounts of solid wastes and wastewater which threaten the quality of the environment and impose an economic burden on their producers and governments. However, the waste contains a variety of fertilizer components and renewable energy sources. Recycling the resources in agriculture and effective utilization of renewable energy would minimize the import of fertilizers and energy which would ensure environmental sustainability and economic viability. This research used aquatic cattail as a feedstock to study the agricultural waste recycling technologies: anaerobic digestion (AD) and biochar production, which provided a research foundation for biorefinery technology that uses agricultural waste to produce energy and fertilizer.

The aquatic plant of cattail (*Typha species*) is a biomass crop that is especially suitable for wetlands.[4] Cattail has high pest resistance and high adaptability. Because of its superiority in productivity (40+ metric ton/ha standing crops), cattail is a potential and plentiful feedstock for AD.[5]

AD is a cost-effective waste treatment technology that produces methane (CH_4, also called biomethane) from almost all organic wastes such as animal manure,[6] crop residues,[7] food wastes[8] and energy corps.[9] Temperature and pH are two of the most important aspects of AD as the growth of microorganisms depends heavily on them. AD can be carried out under mesophilic (25–37 °C) and thermophilic (55–65 °C) conditions. Most of full scale anaerobic digesters are carried out at mesophilic temperature.[10] However, mesophilic anaerobic digesters have longer start up time and moderate rate of lignocellulose degradation.[11] On the other hand, thermophilic temperature results in better degradation of lignocellulosic biomass, thus improving AD efficiency and eradicates pathogens as compared to mesophilic AD. Therefore, thermophilic AD has gained popularity as it provides better efficiency of AD and eradicates pathogens.[12] Hundreds of microbial species are involved in the AD process, where methanogenic bacteria are extremely sensitive to pH. The pH is an indicator of the accumulation

CONTACT Lijun Wang ✉ lwang@ncat.edu 📇 Department of Natural Resources and Environmental Design, North Carolina Agricultural and Technical State University, 1601 East Market Street, Greensboro, NC 27411, USA.
Color versions of one or more of the figures in the article can be found online at www.tandfonline.com/lesa.
© 2019 Taylor & Francis Group, LLC

of volatile fatty acids (VFA) in the system.[13] If a high concentration of VFA is formed, the pH will be lowered to a level that severely inhibits methanogens. Thermophilic AD typically operates at a pH of 6.5–7.5.[14]

During AD, about 30–50% of the organic matter is decomposed, while the remaining 50–70% becomes a large amount of AD digestate which contains digestate solids and effluent (liquid).[15] AD digestate is generally not suitable for direct application on land because it contains a wide range of chemicals and microorganisms that can pollute the environment.[16] Therefore, the recovery of nutrients and water from the AD digestate, before releasing it in the environment, will not only benefit the sustainability of fertilizer and water supply but also alleviate the pollution. Biochar (activated biochar or activated carbon-AC) can be an effective adsorbent to recover nutrients like ammonia (N) and phosphates (P) from AD effluent.[17,18] For large-scale application of AC, the production cost can be reduced by either choosing a cheaper feedstock or applying a proper activation method.[19] The conversion of the digestate into AC would eliminate the need for treating residue and increase the economic value. In addition, extraction and concentration of useful N and P nutrients from the AD effluent, using AC as an adsorbent, could provide an opportunity for sustainable fertilizer production, odor control, pathogen reduction and farm nutrient balance management.

Hydrothermal carbonization (HTC) is a typical biochar production method that is suitable for wet feedstock. HTC obviates the need to dry the raw material, which may be a cost-effective approach for feedstocks with high moisture content like aquatic plants and AD digestate. HTC permits reactions to be carried out at lower temperatures ($<350\,^{\circ}$C) in comparison with pyrolysis (350–650 °C). Low-temperature HTC can mimic the natural process of coalification of biomass, although in HTC the reaction rate is higher and the reaction time is shorter compared to the slow process of natural coalification of biomass which takes up to hundreds of years.[20] Biochar yield after HTC of biomass varies from 30% to 60% depending on the feedstock properties, reaction temperature and pressure.[21] The biochar produced via HTC is often called hydrochar. The physiochemical properties of biochar differ depending on the techniques applied. Previous studies have compared the properties of hydrochar produced via HTC to biochar produced via gasification/pyrolysis and concluded that the hydrochar is superior to biochar because hydrochar contains more functional groups, has reduced alkali, and alkaline earth.[22–24]

A salt melt synthesis (SMS) method was employed in this study to enhance the quality of hydrochar.[25,26] SMS uses molten inorganic salt as the medium for either the reaction or activation step. SMS has emerged as an important complementary route to the conventional liquid phase synthesis over the years. A detailed review of this topic can be found in the literature.[27]

In this study, fresh and dried cattail was anaerobically digested separately at thermophilic temperature and the effect of different particle size on the methane yield was studied. Following AD, HTC was conducted using the cattail digestate. Analysis was run on the HTC products and the effect of AD on these products was carefully studied. To improve the quality of hydrochar, hydrochar was subjected to SMS method using three sodium salts, including sodium carbonate (Na_2CO_3), sodium bicarbonate ($NaHCO_3$), and sodium chloride (NaCl).

Materials and method

Materials

The aerial portions of cattail, *Typha latifolia*, were harvested from the North Carolina Agricultural and Technical State University farm in the summer of 2018. Fresh cattail was cut into 1-in. pieces and was divided into two batches. The first batch was directly used as the feedstock for AD, while the rest was dried naturally at room temperature for at least 2 weeks. Dried cattail was ground to a particle size of ~1 mm by using a Thomas Model 4 Wiley Mill (Thomas Scientific, Swedesboro, NJ, USA) and then stored in an airtight container at room temperature. The solid contents of fresh and dried cattail were $38.7 \pm 1.9\%$ and $92.1 \pm 0.7\%$, respectively. The biomass composition of cattail was presented in our previous publication,[28] which includes 34.5% cellulose, 11.7% xylan, 26.4% Klason lignin and other sugars. Fresh cattail also contains proteins, free amino acids, organic acids, dyes, enzymes, hormones, other organic substances and minerals.[29]

The inoculum for all AD experiments was the effluent which was collected from an previous running anaerobic digester at the University farm.[30] The anaerobic digester digested swine manure with a solid content of 3 wt % under continuous agitation at 250 rpm at 55 °C. The effluent was collected on the day of the experiment and used immediately.

Anaerobic digestion

Fresh cattail (1-in. pieces) and dried cattail (1-in. pieces and fine powder) were anaerobically digested using the Automatic Methane Potential Test System (AMPTS II) (Bioprocess Control, Sweden).[31] For a typical experiment, the biomethane potential test was performed in a 500 mL flask with a working volume of 400 mL, in which ~20 g (dry basis) feedstock was inoculated with 400 mL effluent giving a 0.25 g volatile solids (VS) inoculum/g VS. The experiments were carried out in duplicate or triplicate at 55 °C. The AD of fresh cattail (1-in. pieces) and dried cattail (powdered) was conducted for 14 days. The dried cattail (1-in. pieces) was anaerobically digested for 7 days and 14 days. The biomethane potential was measured daily. The biogas composition was recorded using Biogas 5000 analyzer (Landtech North America, Dexter, MI, USA) and the final pH was measured at the end of the experiment. After the AD process, AD digestate was filtered to yield AD solid digestate (i.e. digested cattail) and the liquid AD effluent.

Kinetic model of biomethane production

The modified Gompertz Equation was used to fit the cumulative methane production data as shown in Eq. (1)[32]:

$$P(t) = Pm * \exp\left\{-\exp\left[\frac{Rm*e}{Pm}\ (\lambda - 1) + 1\right]\right\} \tag{1}$$

where P_m is the maximum CH_4 yield (mL); R_m is the maximum daily methane production (mL); λ is the lag phase (d); $P(t)$ is the cumulative methane yield at time t (mL) and e is the base of natural logarithm. Kinetic parameters of P_m, λ and R_m were determined using non-linear regression in Microsoft Excel (Redmond, WA, USA).

Hydrothermal carbonization

The detailed experimental apparatus of HTC was described in our previous publication.[33] Dried cattails (1-in. pieces) that had been anaerobically digested for 14 days were used as raw materials. The HTC of cattail was also performed to compare the effects of AD. For a typical experiment, 3 g (dry basis) of the feedstock was mixed with 50 mL liquid AD effluent. In case of HTC of cattail, 3 g of cattail was mixed with 50 mL deionized water. This mixture was hydrothermally carbonized in a 75-mL Parr high-pressure reactor (Parr Instrument, Moline, IL, USA). The temperature of the reactor was increased at a heating rate of about 10 °C/min and held at 250 °C for 4 h. The literature has different opinions on the precise reaction conditions of the HTC reaction. It is generally considered that the reaction temperature is between 150 and 350 °C (preferably 180–250 °C) and the reaction time is typically several hours.[34,35] In this study, moderate reaction conditions of 250 °C and 4 h were chosen to prepare hydrochar.

When the reaction was completed, the reactor was cooled down to the room temperature by using a fan that gave a cooling rate of ~10 °C/min. Once the reactor reached the room temperature, the final pressure in the reactor was measured with a digital pressure gauge, and then the gaseous products were collected in a 1-L Tedlar bag for gas chromatography (GC) analysis. Both the final pressure and the composition of the gaseous products were used to calculate the gas weight. The hydrochar was separated from the aqueous fraction by filtration, washed with 50 mL acetone and then dried at 105 °C for 12 h. The acetone soluble fraction was companied with the aqueous products as the liquid products.

The product yield was defined as the following Eqs. (2)–(4):

$$\text{Yield of residue }(\%) = \frac{weight\ of\ solid\ residue}{weight\ of\ dry\ biomass} \times 100\% \tag{2}$$

$$\text{Yield of gas }(\%) = \frac{weight\ of\ gas}{weight\ of\ dry\ biomass} \times 100\% \tag{3}$$

$$\text{Yield of liquid }(\%) = 100\% - \text{ Yield of biochar}(\%) - \text{Yield of gas}(\%) \tag{4}$$

Molten salt activation of hydrochar

Due to their availability and lower cost, the most common molten salts are typically chlorides, sulfates, carbonates and hydroxides. Ensuring safety and minimizing environmental pollution, the following three sodium salts were chosen: Na_2CO_3, $NaHCO_3$ and NaCl. In a typical process, hydrochar was mixed with one salt in a ratio of 1:3, and then the mixture was homogenized with a mortar and pestle. The powdered mixture was transferred to a ceramic crucible and was placed in an electric furnace equipped with a continuous nitrogen flow. After flushing with nitrogen for 30 min, the furnace was ramped at 10 °C/min to the carbonization temperature of 900 °C and kept at this temperature for 1 h. The furnace was cooled to ambient temperature by switching off the power; meanwhile, the nitrogen flow was maintained until the temperature reached room temperature. The as-obtained product (i.e. activated hydrochar) was crushed into particles using a mortar and pestle and washed with sufficient amount of water to remove the salts. The activated hydrochar was dried in an oven at 105 °C for 12 h.

Characterization

Chemical compositions of the liquid products generated from HTC were analyzed using an Agilent 7890–5975 °C gas chromatography-mass spectrometry (GC/MS) (Santa Clara, CA, USA) with a DB-1 column. The GC was programed to hold the temperature at 40 °C for 2 min and was gradually increased at the rate of 10 °C/min to attain a temperature of 250 °C and was held for 10 min. The injector temperature was 300 °C, and the injection volume was 1 μl. The flow rate of the carrier gas (helium) was 0.6 mL/min. The ion source temperature was 300 °C for the mass selective detector. The compounds were identified with a comparison to the Mass Spectral Database of the National Institute of Standards and Technology (USA).

Gaseous products generated during HTC were analyzed by using a Varian CP-4900 Micro-GC (Santa Clara, CA, USA) with MS5A, PPQ and WAX columns and a thermal conductivity detector for the analysis of hydrogen, carbon monoxide, carbon dioxide, methane and other gases.

To obtain the morphology of the feedstocks and hydrochar, scanning electron microscopy (SEM) images were acquired on a JEOL JSM-7600F scanning electron microscope (Tokyo, Japan) operated at a 5 kV accelerating potential provided with an in-lens detector. Elemental composition of samples was determined by using the same SEM with the energy-dispersive X-ray detector operated at a 20 kV accelerating potential.

To compare the specific surface area and pore size in samples, physical adsorption was measured with a Micromeritics ASAP 2020 surface area and porosity analyzer (Norcross, GA, USA).

Results and discussion

Thermophilic anaerobic digestion of cattail

Cattail was anaerobically digested with 5% solid content and at a thermophilic temperature of 55 °C. Fresh cattail (1-in. pieces) and dried cattail (fine powder) was digested for

Table 1. Experimental results of cattail AD and kinetic parameters of cumulative methane production using modified Gompertz Model.

	Experimental results				Kinetic parameters		
Feedstock and AD period	Methane yield (mL/g VS)	Mass reduction	pH after AD	Cumulative methane yield (mL)	P_m (mL)	R_m (mL)	λ (day)
Fresh 1-in. (14-day)	203 ± 13	55.7%	7.8	957.2	4432	115.1	4.5
Dried Fine powder (14-day)	275 ± 15	36.5%	7.5	1160	1184	130.8	0
Dried 1-in.(14-day)	258 ± 24	33.2%	7.3	1039	1330	94.1	1.48
Dried 1-in.(7-day)	196 ± 7	18.9%	7.1	487	2447	70.7	2.15

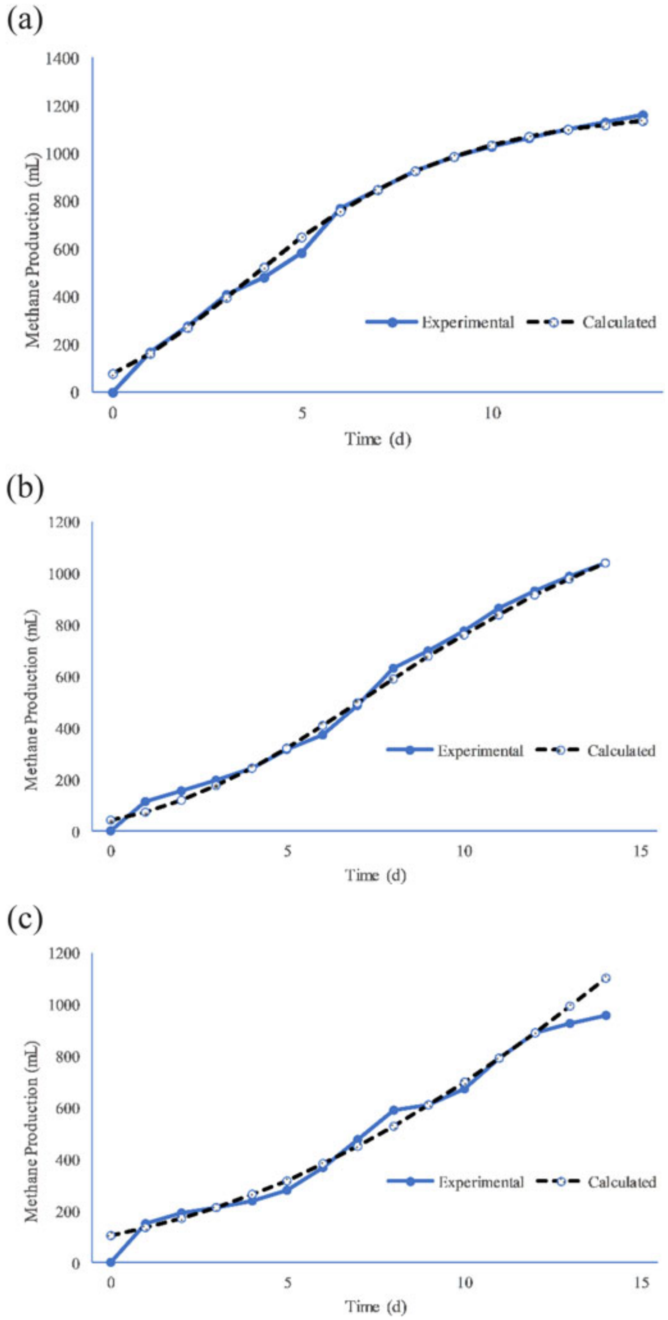

Fig. 1. Experimental and calculated biomethane production during the 14-day AD of (a) cattail in the form of dry fine power, (b) dry 1-in. cattail pieces and (c) fresh cattail.

14 days only while dried cattail (1-in. pieces) was digested for 7-day and 14-day. The biogas produced consisted of about 60 vol % CH_4, while the CO_2 content was approximately 38 vol %, with the balance of hydrogen sulfide, nitrogen and oxygen. The cumulative methane production was fitted in the modified Gompertz equation. The experimental and modeling results are compared in Table 1 and Figure 1.

As shown in Table 1, for a 14-day digestion, the average methane production of dried cattails and fresh cattails was 258–275 and 203 mL/g VS, respectively. The total solid (TS) reduction of dried cattail and fresh cattail was 33–36% and 55.7%, respectively. The pH values at the end of experiments were between 7.1 and 7.8. The use of fresh cattails resulted in a higher pH and a lower methane yield compared to dried cattail, probably due to the presence of bioactive compounds in fresh cattails. As analyzed in our previous publication, fresh cattail contains amino acids, organic acids and some other metabolites.[29] Since healthy thermophilic AD requires a pH between 6.5 and 7.5, digesting cattail under different conditions still requires careful pH control.

The cumulative biomethane production from the current experimental set-up (400 mL working volume with 5% solid content) was 957, 1039–1163 and 487 for 14-day AD of fresh cattail, 14-day AD of dried cattail and 7-day AD of dried cattail (1-in. pieces), respectively (Table 1). It was observed that the modified Gompertz model was suitable to describe the biomethane production of 14-day AD of dried cattail, because the calculated values of P_m were close to the experimental results. It was also found that the biomethane production calculated under the condition of dried cattail AD is in good agreement with the experimental value (Fig. 1). The lag phases of the 14-day AD of dried fine powder and 1-in. pieces were 0 and 1.8 days, respectively. Therefore, the use of the feedstock with a smaller particle size could reduce the length of the lag phase. In the case of fresh cattail AD and 7-day AD, the model gave these two conditions a long lag phase and a very high maximum methane yield, indicating a slow and incomplete digestion process.

HTC of cattail and digested cattail

HTC of cattail was done with DI water, while HTC of anaerobically digested cattail (dried, 1-in. pieces and 14-day AD) was conducted with the liquid AD effluent. The yields of non-condensable gases, liquid products and hydrochar from these processes are summarized in Table 2. A small amount (3.3–7.5 wt %) of gaseous products was produced during the HTC process. The major gas component was CO_2, which accounted for 83–89 vol % of the total gaseous products, and the remaining balance was 1–2 vol % H_2, 7–13.5 vol % CO, 0.1–0.36 vol % CH_4, etc. (Table 3).

Because the AD effluent was used as the reaction reagent, H_2S (>5000 ppm) generated during the AD process also entered the gaseous phase.

The majority products of these HTC processes were liquid chemicals including water-solubles and acetone-solubles. A list of GC/MC detectable chemicals is given in Table 4. Because the cattail was harvested in the summer, it contained protein and other metabolites in addition to cellulosic components, therefore, the liquid products from HTC of cattail contained several nitrogenated compounds such as (1-methylethyl)-hydrazine, pyridine, ethanethioamide and o-isopropylhydroxylamine. Products such as aldehydes, ketones and alcohols are usually derived from the degradation of cellulose and hemicellulose, while phenolic derivatives are derived from the degradation of lignin.

The process of AD had an effect on the liquid products of HTC. The ratio of the nitrogenated chemicals in the liquid products of HTC of digested cattail was lower than that of original cattail. Because nitrogenated chemicals are the degradation products of proteins, the result indicates that the protein of cattail was partially degraded during AD. The total number of chemical species in the liquid products of HTC of digested cattail was also lower than that of original cattail, which may be due to the degradation of cellulose and hemicellulose in cattail during AD. Meanwhile, the ratio of phenolic derivatives in the liquid products obtained via HTC of the digested cattail was higher than that of original cattail, confirming that lignin is non-digestible material. Because the HTC reaction temperature of 250 °C is relatively low for complete degradation of biomass into monomers, only limited organic chemicals in the liquid products can be identified by GC/MS.

Table 2. Product yields of HTC of cattail and digested cattails at 250 °C and 4 h.

Yields (wt %)	Cattail	7-day AD	14-day AD
Gas	3.3 ± 0.3	6.7 ± 1.3	7.5 ± 1.5
Liquid[a]	69.0	64.3	64.3
Biochar	27.7 ± 0.7	28.8 ± 0.5	28.2 ± 1.1

[a]The liquid yield was calculated according to Eq. (4).

Table 3. The composition of gaseous products of HTC.

Gas component (vol %)	Cattail	7-day AD	14-day AD
H_2	1.08	1.32	1.77
CO	7.82	10.53	13.54
CH_4	0.13	0.12	0.36
CO_2	89.36	87.43	83.69
H_2S	–	0.55	0.63

–: not detectable.

The yield of solid residues of HTC (i.e. hydrochar) was ~28 wt %. Table 5 shows elemental analyses of cattail, digested cattail (dried 1-in. pieces) and hydrochar. The carbon (C) content in cattail was about 72%. After AD, the C content was reduced to around 63% due to the conversion of carbon into methane and carbon dioxide. HTC of cattail increased the C content to almost 80%, while HTC of digested cattail increased the C contents to ~77%. Besides C, hydrochar contained 20–22% oxygen (O) and ~1% calcium (Ca). Phosphorus (P) existing in some samples may originate from the AD process.

The morphology of cattail, digested cattail (dried 1-in. pieces) and hydrochar were revealed via SEM analysis. These three samples were magnified about 50,000 times, and the scale in Figure 2 was 200 nm. The surface of cattail showed its characteristic texture (Fig. 2a). After 14-day digestion, there was no obvious change in the surface of cattail (Fig. 2b). However, after carbonization, it was noticeable that the texture characteristic of cattail had disappeared from the surface of the hydrochar (Fig. 2c). The material

Table 4. GC/MS analysis of liquid products of HTC of cattail and digested cattails (area %).

Retention time (min)	Possible chemicals	Cattail	7-day AD	14-day AD
1.63	Hydrazine, (1-methylethyl)-	1.5	1.4	0.4
1.73	Pyridine	4.0	1.2	1.1
1.92	2-Butanone	1.6	3.4	0.8
1.97	Ethane, 1,1-dimethoxy-	1.9	–	–
2.47	Propanal, 3-methoxy-	1.1	–	–
2.84	Propane, 1,1-dimethoxy-	0.9	0.9	–
3.64	Propane, 1,1-dimethoxy-2-methyl-	1.0	0.2	–
4.07	Cyclopentanone	2.4	5.0	2.0
4.99	2-Cyclopenten-1-one, 2-hydroxy-	1.2	2.6	0.7
5.07	Cyclopentanone, 3-methyl-	0.6	1.3	0.5
5.28	Ethanethioamide	0.6	0.7	–
5.38	o-Isopropylhydroxylamine	1.0	0.6	–
6.14	2-Cyclopenten-1-one, 2-methyl-	4.7	6.1	1.7
6.77	2-Butynoic acid	0.6	1.1	
7.78	2-Cyclopenten-1-one, 2,3-dimethyl-	2.2	4.2	3.2
8.45	2-Cyclopenten-1-one, 3-ethyl-	4.1	4.7	2.9
9.3	2-Cyclopenten-1-one, 3,4,4-trimethyl-	1.9	2.6	2.2
9.36	Phenol, 2-methoxy-	9.0	11.3	16.2
10.48	1-Butanol, 2-ethyl-	2.9	0.8	1.9
10.68	Phenol, 3-ethyl-	1.5	–	–
10.99	Creosol	3.3	6.1	7.4
11.24	Decanal	2.8	–	–
12.25	Phenol, 4-ethyl-2-methoxy-	9.5	15.9	14.9
13.07	Phenol, 2,6-dimethoxy-	21.9	11.5	23.1
14.36	1,2,3-Trimethoxybenzene	3.1	1.6	1.6
15.35	Phenol, 2,5-bis(1,1-dimethylethyl)-	12.7	12.5	13.4
16.36	6-Ethyl-3-propionyl-2,3-dihydropyran-2,4-dione	2.0	4.2	6.2

–: not detectable.

Table 5. Elemental analysis of cattail, digested cattails and hydrochar.[a]

	Feedstock			Hydrochar		
Element	Cattail	7-day AD	14-day AD	Cattail	7-day AD	14-day AD
C	72.18	62.71	63.53	79.79	76.84	77.55
O	26.03	35.56	29.51	19.97	22.28	20.97
K	1.43	–	–	0.23	–	–
Ca	–	0.18	0.27	0.91	0.88	1.07
Mg	–	0.44	–	–	–	–
P	–	0.36	0.17	–	–	0.42

[a]For each sample, 5–10 particles were analyzed, and average values were reported.

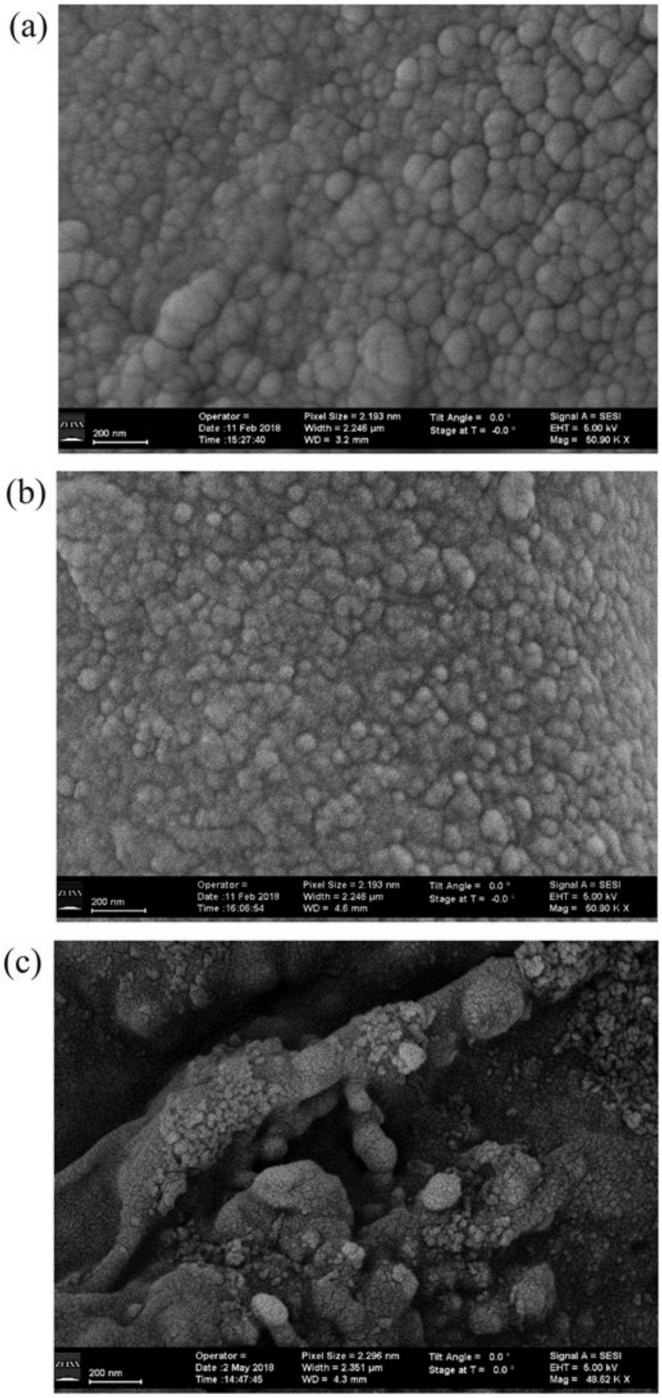

Figure 2. SEM analysis of (a) cattail, (b) cattail anaerobically digested for 14 days and (c) hydrochar produced from (b).

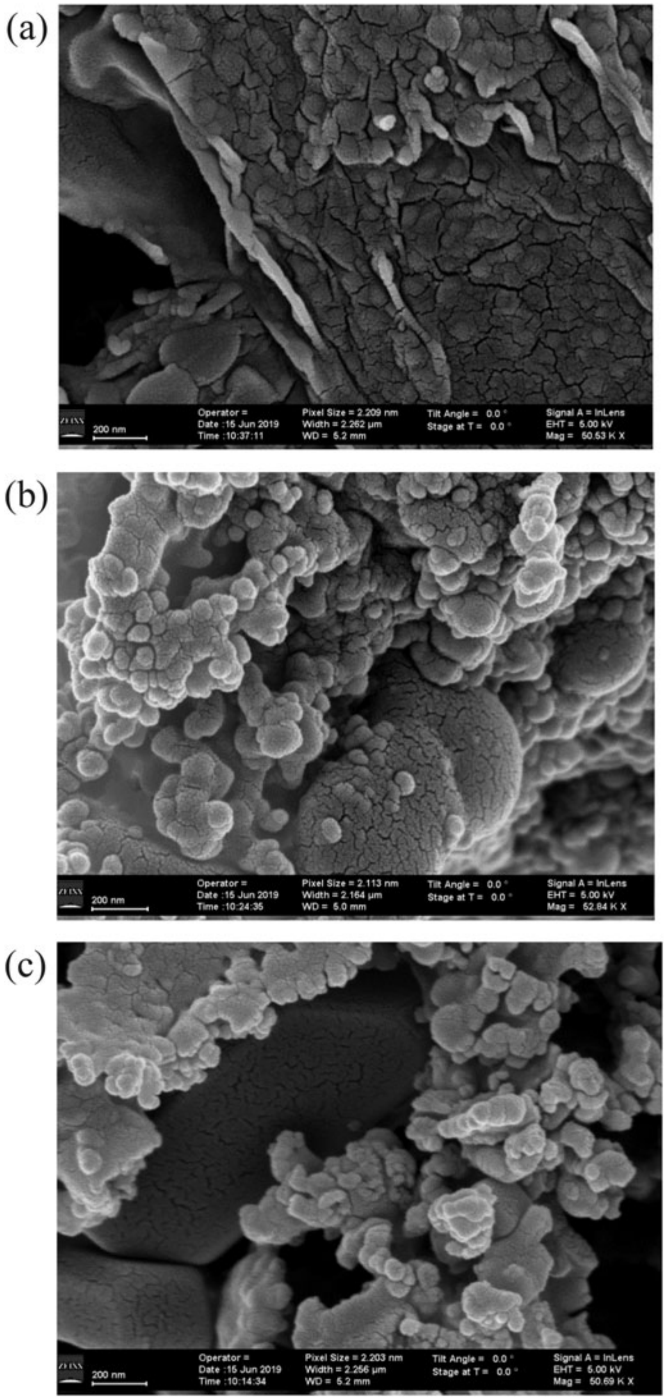

Figure 3. SEM analysis of hydrochar activated by using (a) Na_2CO_3, (b) $NaHCO_3$ and (c) NaCl.

Table 6. Surface area and porosity analyses of cattail, digested cattails and hydrochar.

		Digested cattail		Hydrochar			Activated hydrochar		
Characteristics	Cattail	7-day AD	14-day AD	Cattail	7-day AD residues	14-day AD residues	Na_2CO_3	$NaHCO_3$	NaCl
BET Surface area (m^2/g)	0.4505	0.431	0.4165	10.09	9.48	10.08	628.49	441.09	251.73
t-Plot micropore area (m^2/g)	–	–	0.218	0.13	0.06	0.03	422.67	286.59	182.45
t-Plot micropore volume(cm^3/g)	–	–	0.00008	–	–	–	0.198	0.1344	0.0855
Meso pore volume(cm^3/g)	0.001	–	0.0011	0.0327	0.0314	0.045	0.238	0.235	0.044
Average pore width(nm)	10.7	–	12.49	13.2	17.2	18.5	3.22	3.76	2.5

Table 7. SEM-EDX analysis of activated hydrochar.

Element	Na_2CO_3	$NaHCO_3$	NaCl
C	93.57	89.73	82.48
O	5.11	6.1	8.56
Ca	0.3	1.85	5.36
Al	0.05	0.05	0.04
Mg	0.03	0.08	0.17
P	0.13	0.95	1.88
Ni	0.16	0.51	0.74
S	0.06	0.14	0.46
Na	0.63	0.59	0.17
Cl	–	–	0.14

turned black and had carbon particles of different sizes on the surface.

Surface area and porosity analyses of the feedstocks and hydrochar are summarized in Table 6. Cattail possessed a very low surface area. Although AD degraded the feedstock partially, the BET (Brunauer-Emmett-Teller) specific surface areas of digested cattail (dried 1-in. pieces) were still negligible and lower than $0.45\,m^2/g$. It was evident that the 14-day AD created a small number of micropores in this material. HTC of cattail or digested cattail further increased the BET specific surface area of hydrochar to $\sim 10\,m^2/g$ with only trace amounts of micropore area.

Melting salt activation of hydrochar and its application

Hydrochar produced from the 14-day AD digestate of dried cattail (1-in. pieces) was further activated by using three sodium salts of Na_2CO_3, $NaHCO_3$, and NaCl at 900 °C. The surface of activated hydrochar showed more gaps and more carbon particles (Fig. 3). The BET specific surface areas of activated hydrochar were approximately 630, 440 and $250\,m^2/g$ for the application of Na_2CO_3, $NaHCO_3$ and NaCl, respectively. The micropore area accounted for 64–72% of total surface area. Activation process increased the C content of hydrochar to 84.4–93.5% with the balance being 5–8.6% O, 0.1–1.9% P and trace amounts of other elements like Ca, Al, Mg, Ni, S, etc. (Table 7).

The melting points of Na_2CO_3 and NaCl are 851 and 801 °C, respectively. The melting point of sodium bicarbonate ($NaHCO_3$) is any temperature over 50 °C because it starts to undergo thermal decomposition, forming sodium carbonate (Na_2CO_3), water and carbon dioxide. Three molten salts behaved differently during carbonization. However, the mechanism for formation of porosity in molten salts is still unclear. Some publications attribute the formation of activated carbon to the templating action of intentionally added salts during the synthesis,[36,37] while others considered carbonates as both template and activating agent.[38] According to the experimental results, it can be clearly seen that sodium carbonate is the optimum activating agent, and the hydrochar activated by Na_2CO_3 had the highest specific surface area. Sodium carbonate is more economical and safer than activators commonly used in industrial production such as KOH and $ZnCl_2$.

The proposed applications for the activated hydrochar include phosphorus adsorption in wastewater or AD effluent and carbon dioxide adsorption. However, when all the activated hydrochars synthesized in this study were compared with commercially available activated carbon (Catalog # 242276, Sigma Aldrich, USA), all materials including commercially available activated carbon showed similar and low adsorption capacity. The results indicated that the physical adsorption capacity of activated hydrochar for carbon dioxide (<0.1 mg/g hydrochar) and phosphorus (<5 mg/g hydrochar) was very low. To improve the chemical adsorption capacity of the activated hydrochar, further surface modification such as loading magnesium is required.[39]

Conclusion

The cattail was anaerobically digested at 55 °C for 14 days, partially degrading its protein and cellulose components. The average methane yield was 230–280 mL/g VS, and the total solids reduction was 33–55%. When using fresh cattail as a feedstock, careful control of the pH during AD is required. Reducing the particle size prior to AD might reduce the length of the lag phase. A 14-day AD process could create a small number of micropores in the cattail AD digestate. Hydrothermal carbonization of this AD digestate yielded approximately 6.7–7.5% gases, 28% hydrochar and 64% liquid products. Due to the AD process, HTC gaseous products contained >5000 ppm H_2S and liquid products possessed fewer chemical species but a higher ratio of phenolic compounds compared to the liquid products from HTC of original cattail. The hydrochar had a higher carbon content (76.8–79.8%) and a higher specific surface area ($\sim 10\,m^2/g$) than those of the feedstock which had a carbon content of 63–72% and a specific surface area of $<0.45\,m^2/g$. Hydrochar was further activated by using three sodium salts of Na_2CO_3, $NaHCO_3$, and NaCl. Activation process increased the C content of hydrochar to 84–93% and the BET specific surface area to $250–630\,m^2/g$. Further surface modification is required to improve the absorption ability of the activated hydrochar.

Funding

The publication was made possible by the United States Department of Agriculture (USDA National Institute of Food and Agriculture (NIFA) award: NC.X-314-5-18-130-1). This work was partially performed at the Joint School of Nanoscience and Nanoengineering, a member of Southeastern Nanotechnology Infrastructure Corridor (SENIC) and National Nanotechnology Coordinated Infrastructure (NNCI), which is supported by the National Science Foundation (ECCS-1542174).

References

[1] Barthel, S.; Isendahl, C. Urban Gardens, Agriculture, and Water Management: Sources of Resilience for Long-Term Food Security in Cities. *Ecol. Econ.* **2013**, *86*, 224–234. DOI: 10.1016/j.ecolecon.2012.06.018.

[2] Rojas-Valencia, M. N.; Velásquez, M. T. O. d.; Franco, V. Urban Agriculture, Using Sustainable Practices that Involve the Reuse of Wastewater and Solid Waste. *Agric. Water Manage.* **2011**, *98*, 1388–1394. DOI: 10.1016/j.agwat.2011.04.005.

[3] Bekoe, D.; Wang, L.; Zhang, B.; Todd, M. S.; Shahbazi, A. Aerobic Treatment of Swine Manure to Enhance Anaerobic Digestion and Microalgal Cultivation. *J. Environ. Sci. Health, Part B* **2018**, *53*, 145–151. DOI: 10.1080/03601234.2017.1397454.

[4] Zhang, B.; Shahbazi, A.; Wang, L.; Diallo, O. The Pretreatment, Enzymatic Hydrolysis, and Fermentation of Cattails from Constructed Wetlands. *Energy Sourc. Part A* **2013**, *35*, 246–252. DOI: 10.1080/15567036.2010.509089.

[5] Hu, Z.-H.; Yu, H.-Q. Anaerobic Digestion of Cattail by Rumen Cultures. *Waste Manage.* **2006**, *26*, 1222–1228. DOI: 10.1016/j.wasman.2005.08.003.

[6] Holm-Nielsen, J. B.; Al Seadi, T.; Oleskowicz-Popiel, P. The Future of Anaerobic Digestion and Biogas Utilization. *Bioresour. Technol.* **2009**, *100*, 5478–5484. DOI: 10.1016/j.biortech.2008.12.046.

[7] Neshat, S. A.; Mohammadi, M.; Najafpour, G. D.; Lahijani, P. Anaerobic co-Digestion of Animal Manures and Lignocellulosic Residues as a Potent Approach for Sustainable Biogas Production. *Renew. Sustain. Energy Rev.* **2017**, *79*, 308–322. DOI: 10.1016/j.rser.2017.05.137.

[8] Zhang, C.; Su, H.; Baeyens, J.; Tan, T. Reviewing the Anaerobic Digestion of Food Waste for Biogas Production. *Renew. Sustain. Energy Rev.* **2014**, *38*, 383–392. DOI: 10.1016/j.rser.2014.05.038.

[9] Zhang, B.; Wang, L.; Li, R. Production of Biogas from Aquatic Plants. In *Aquatic Plants: Composition, Nutrient Concentration and Environmental Impact*; Rodney, C.E., Ed.; New York: Nova Science Publishers, **2015**; pp 33–46.

[10] Yenigün, O.; Demirel, B. Ammonia Inhibition in Anaerobic Digestion: A Review. *Process Biochem.* **2013**, *48*, 901–911. DOI: 10.1016/j.procbio.2013.04.012.

[11] Yang, L.; Xu, F.; Ge, X.; Li, Y. Challenges and Strategies for Solid-State Anaerobic Digestion of Lignocellulosic Biomass. *Renew. Sustain. Energy Rev.* **2015**, *44*, 824–834. DOI: 10.1016/j.rser.2015.01.002.

[12] Sasaki, D.; Hori, T.; Haruta, S.; Ueno, Y.; Ishii, M.; Igarashi, Y. Methanogenic Pathway and Community Structure in a Thermophilic Anaerobic Digestion Process of Organic Solid Waste. *J. Biosci. Bioeng.* **2011**, *111*, 41–46.

[13] Zhang, B.; Wang, Y. *Biomass Processing, Conversion and Biorefinery*; New York: Nova Science Publishers, Inc., **2013**.

[14] Nishio, N.; Nakashimada, Y. Chapter 7 – Manufacture of Biogas and Fertilizer from Solid Food Wastes by Means of Anaerobic Digestion. In *Food Industry Wastes*; Kosseva, M. R., Webb, C. Eds.; Academic Press; San Diego, **2013**; pp 121–133.

[15] Zhang, B.; Li, Y.; Li, S.; Li, G.; Sun, Q. Effect of Inoculated and Uninoculated Aeration Pretreatment on Nutrients and Phytotoxicity of Anaerobic Digestion Effluent. *Sci. Rep.* **2018**, *8*, 13872. DOI: 10.1038/s41598-018-32141-7.

[16] Mata-Alvarez, J.; Macé, S.; Llabrés, P. Anaerobic Digestion of Organic Solid Wastes. An Overview of Research Achievements and Perspectives. *Bioresour. Technol.* **2000**, *74*, 3–16. DOI: 10.1016/S0960-8524(00)00023-7.

[17] Rodrigues, C. C.; de Moraes, D.; da Nóbrega, S. W.; Barboza, M. G. Ammonia Adsorption in a Fixed Bed of Activated Carbon. *Bioresour. Technol.* **2007**, *98*, 886–891. DOI: 10.1016/j.biortech.2006.03.024.

[18] Jayson, G. G.; Lawless, T. A.; Fairhurst, D. The Adsorption of Organic and Inorganic Phosphates onto a New Activated Carbon Adsorbent. *J. Colloid Interface Sci.* **1982**, *86*, 397–410. DOI: 10.1016/0021-9797(82)90085-6.

[19] Dias, J. M.; Alvim-Ferraz, M. C. M.; Almeida, M. F.; Rivera-Utrilla, J.; Sánchez-Polo, M. Waste Materials for Activated Carbon Preparation and Its Use in Aqueous-Phase Treatment: A Review. *J. Environ. Manage.* **2007**, *85*, 833–846. DOI: 10.1016/j.jenvman.2007.07.031.

[20] Xiu, S.; Shahbazi, A.; Li, R. Characterization, Modification and Application of Biochar for Energy Storage and Catalysis: A Review. *Tr. Ren. Energy* **2017**, *3*, 86–101. DOI: 10.17737/tre.2017.3.1.0033.

[21] Titirici, M.-M.; White, R. J.; Falco, C.; Sevilla, M. Black Perspectives for a Green Future: Hydrothermal Carbons for Environment Protection and Energy Storage. *Energy Environ. Sci.* **2012**, *5*, 6796–6822. DOI: 10.1039/c2ee21166a.

[22] Wiedner, K.; Rumpel, C.; Steiner, C.; Pozzi, A.; Maas, R.; Glaser, B. Chemical Evaluation of Chars Produced by Thermochemical Conversion (Gasification, Pyrolysis and Hydrothermal Carbonization) of Agro-Industrial Biomass on a Commercial Scale. *Biomass Bioenergy* **2013**, *59*, 264–278. DOI: 10.1016/j.biombioe.2013.08.026.

[23] Kambo, H. S.; Dutta, A. A Comparative Review of Biochar and Hydrochar in Terms of Production, Physico-Chemical Properties and Applications. *Renew. Sustain. Energy Rev.* **2015**, *45*, 359–378. DOI: 10.1016/j.rser.2015.01.050.

[24] Taskin, E.; de Castro Bueno, C.; Allegretta, I.; Terzano, R.; Rosa, A. H.; Loffredo, E. Multianalytical Characterization of Biochar and Hydrochar Produced from Waste Biomasses for Environmental and Agricultural Applications. *Chemosphere* **2019**, *233*, 422–430. DOI: 10.1016/j.chemosphere.2019.05.204.

[25] Liu, X.; Antonietti, M. Moderating Black Powder Chemistry for the Synthesis of Doped and Highly Porous Graphene Nanoplatelets and Their Use in Electrocatalysis. *Adv. Mater.* **2013**, *25*, 6284–6290. DOI: 10.1002/adma.201302034.

[26] Liu, X.; Giordano, C.; Antonietti, M. A Facile Molten-Salt Route to Graphene Synthesis. *Small* **2014**, *10*, 193–200. DOI: 10.1002/smll.201300812.

[27] Liu, X.; Fechler, N.; Antonietti, M. Salt Melt Synthesis of Ceramics, Semiconductors and Carbon Nanostructures. *Chem. Soc. Rev.* **2013**, *42*, 8237–8265. DOI: 10.1039/C3CS60159E.

[28] Zhang, B.; Shahbaz, A.; Wang, L.; Whitmore, A.; Riddick, B. A. Fermentation of Glucose and Xylose in Cattail Processed by Different Pretreatment Technologies. *BioResources* **2012**, *7*, 2848–2859.

[29] Rahman, Q. M.; Wang, L.; Zhang, B.; Xiu, S.; Shahbazi, A. Green Biorefinery of Fresh Cattail for Microalgal Culture and Ethanol Production. *Bioresour. Technol.* **2015**, *185*, 436–440. DOI: 10.1016/j.biortech.2015.03.013.

[30] Joseph, G.; Zhang, B.; Rahman, Q. M.; Wang, L.; Shahbazi, A. Two-Stage Thermophilic Anaerobic Co-Digestion of Corn Stover and Cattle Manure to Enhance Biomethane Production. *J. Environ. Sci. Health, Part A* **2019**, *54*, 452–460. DOI: 10.1080/10934529.2019.1567156.

[31] Wang, B.; Ivo Achu, N.; Nistor, M.; Liu, J. Determination of Methane Yield of Cellulose Using Different Experimental Setups. *Water Sci. Technol.* **2014**, *70*, 599–604. DOI: 10.2166/wst.2014.275.

[32] Wang, M.; Zhou, J.; Yuan, Y.-X.; Dai, Y.-M.; Li, D.; Li, Z.-D.; Liu, X.-F.; Zhang, X.-Y.; Yan, Z.-Y. Methane Production Characteristics and Microbial Community Dynamics of Mono-Digestion and co-Digestion Using Corn Stalk and Pig Manure. *Int. J. Hydrogen Energy* **2017**, *42*, 4893–4901.

[33] Zhang, B.; Wang, L.; Li, R.; Rahman, Q. M.; Shahbazi, A. Catalytic Conversion of Chlamydomonas to Hydrocarbons via the Ethanol-Assisted Liquefaction and Hydrotreating Processes. *Energy Fuels* **2017**, *31*, 12223–12231. DOI: 10.1021/acs.energyfuels.7b02080.

[34] Biller, P.; Ross, A. B. 17 – Production of biofuels via hydrothermal conversion. In *Handbook of Biofuels Production*, 2nd ed.; Luque, R., Lin, C. S. K., Wilson, K., Clark, J. Eds.; Duxford, UK: Woodhead Publishing, **2016**; pp 509–547.

[35] Mašek, O. 21 - Biochar in Thermal and Thermochemical Biorefineries – Production of Biochar as a Coproduct. In *Handbook of Biofuels Production*, 2nd ed.; Luque, R., Lin, C. S. K., Wilson, K., Clark, J. Eds.; Duxford, UK: Woodhead Publishing, **2016**; pp 655–671.

[36] Fechler, N.; Fellinger, T.-P.; Antonietti, M. "Salt Templating": A Simple and Sustainable Pathway toward Highly Porous Functional Carbons from Ionic Liquids. *Adv. Mater.* **2013**, *25*, 75–79. DOI: 10.1002/adma.201203422.

[37] Lu, A.-H.; Li, W.-C.; Schmidt, W.; Schüth, F. Fabrication of Hierarchically Structured Carbon Monoliths via Self-Binding and Salt Templating. *Microporous Mesoporous Mater.* **2006**, *95*, 187–192. DOI: 10.1016/j.micromeso.2006.05.024.

[38] Díez, N.; Ferrero, G. A.; Fuertes, A. B.; Sevilla, M. Sustainable Salt Template-Assisted Chemical Activation for the Production of Porous Carbons with Enhanced Power Handling Ability in Supercapacitors. *Batteries Supercaps* **2019**, *2*, 701–711. DOI: 10.1002/batt.201900037.

[39] Jiang, Y.-H.; Li, A.-Y.; Deng, H.; Ye, C.-H.; Wu, Y.-Q.; Linmu, Y.-D.; Hang, H.-L. Characteristics of Nitrogen and Phosphorus Adsorption by Mg-Loaded Biochar from Different Feedstocks. *Bioresour. Technol.* **2019**, *276*, 183–189. DOI: 10.1016/j.biortech.2018.12.079.